SF2A 2011
G. Alecian, K. Belkacem, R. Samadi and D. Valls-Gabaud (eds)

THE PHYSICAL PARAMETERS OF THE LOW-MASS MULTIPLE SYSTEM LHS1070 FROM SPECTRAL SYNTHESIS ANALYSIS

A. S. Rajpurohit[1], C. Reylé[1], M. Schultheis[1], C. Leinert[2] and F. Allard[3]

Abstract. LHS1070 is a nearby multiple systems of low mass stars. It is an important source of information for probing the low mass end of the main sequence, down to the hydrogen-burning limit. The primary of the system consist of a mid-M dwarf and two components are late-M to L dwarf, at the star-brown dwarf transition. It makes it even more valuable to understand the formation of dust in cool stellar atmospheres.This work aims to determine the fundamental parameters of LHS1070 and to test recent model atmospheres.We compared the well calibrated data in the optical and infra-red with synthetic spectra computed from recent cool stars atmosphere models. We derived the physical parameters T_{eff}, radius and log g for three components of LHS1070. The models which include the formation and settle of dust are able to reproduce and describe the main features of the visible to IR spectra of the components.

Keywords: stars: atmospheres, stars: fundamental parameters, stars: low-mass

1 Introduction

M dwarfs are the most numerous stars in our Galaxy which makes them an important probe for our galaxy as they carry fundamental informations regarding the stellar physics, galactic structure and formation, and its dynamics. In addition the existence of brown dwarfs or planets being discovered and confirmed around M-dwarfs (Butler et al. 2004; Bonfils et al. 2005) plays an important role for the knowledge of the formation of brown dwarfs and planets. The energy distribution in these late type stars is governed by various absorption molecular bands like TiO, CaH, VO in the optical and H_2O and CO bands in the infrared. The presence of these molecular bands dominates the spectrum in the visible and infared. This affects the resulting opacity in the photosphere of these stars and leads to an onset of the dust formation in the photospheric layers (Tsuji et al. 1996a,b; Allard et al. 1998). In particular, the wavelength region from 6300 Å to 9000 Å encompasses a number of TiO and VO bands which are blended with other lines and leaves no window on the true continuum. Because of their complex atmosphere, a reliable way to determine the physical parameters of M-dwarfs is to compare the observed spectra with synthetic spectra. Atmospheric modeling allows us to determine the fundamental reason for such changes in the cool atmosphere and also helps to determine the physical parameters of the M-dwarfs (Bean et al. 2006).
LHS1070 is a low mass multiple system of cool dwarfs discovered by Leinert et al. (1994), with visual magnitude 15. It is located at a distance of 7.72±0.15 pc from the Sun (Costa et al. 2005) and is considered as a member of the old disk population with a probable age of several Ga (Leinert et al. 2001). The spectral type for the A, B and C components was found to be M5.5-M6, M8.5 and M9-M9.5 (Leinert et al. 2000). Components A,B, and C were the faintest stars within 10 pc from the Sun for which dynamical determinations of mass appeared possible. Leinert et al. (2001); Seifahrt et al. (2008) constrained the combined mass of components B and C and showed that their mass is very close to the hydrogen burning minimum mass, in good agreement with the masses of 0.080-0.083$M_\odot$ and 0.079-0.080$M_\odot$ derived by Leinert et al. (2000) from theoretical mass-luminosity relations (Baraffe et al. 1998; Chabrier et al. 2000).

[1] Université de Franche Comté, Institut UTINAM CNRS 6213, Observatoire des Sciences de l'Univers THETA de Franche-Comté, Observatoire de Besançon, BP 1615, 25010 Besançon Cedex, France.

[2] Max-Planck-Institut für Astronomie, Königstuhl 17, 69117 Heidelberg, Germany.

[3] Centre de Recherche Astrophysique de Lyon, UMR 5574: CNRS, Université de Lyon, École Normale Supérieure de Lyon, 46 allée d'Italie, F-69364 Lyon Cedex 07, France.

The mass range spanned by the components of LHS1070 makes it a valuable system to study, for understanding the formation of dust in the cool atmospheres and the processes that occur at the star/brown dwarf transition. The comparison of the observed spectra of this system with recent atmospheric models helps to determine the stellar parameters (effective temperature, log g, metallicity, radius) and provides an unique opportunity to better understand the lower end of the main sequence which is still poorly understood. LHS1070 is also a testbed to validate and define further developments of the atmospheric models.

2 Model Atmospheres

In this study, we have used the recent new BT-Settl models (Allard et al. 2010) for our analysis of LHS1070. Theses model atmospheres are computed with the PHOENIX code using hydrostatic equilibrium, convection using the Mixing Length Theory and a mixing length of l/Hp=2.0 according to results of radiation hydrodynamics (Ludwig et al. 2006), spherically symmetric radiative transfer, departure from LTE for all elements up to iron, the latest solar abundances by (Asplund et al. 2009), equilibrium chemistry, an important database of the latest opacities and thermochemical data for atomic and molecular transitions, and monochromatic dust condensates refractory indexes. Grains are assumed spherical and non-porous, and their Rayleigh and Mie reflective and absorptive properties are considered. The diffusive properties of grains are treated based on 2-D radiation hydrodynamic simulations, including forsterite cloud formation to account for the feedback effects of cloud formation on the mixing properties of these atmospheres Freytag et al. (2010). For this paper, we use the model grid described as follows: T_{eff} from 2000 K to 4000 K with 100 K step, log g = 5.0 dex, 5.5 dex, M/H = -1.5 dex, -1.0 dex, -0.5 dex, 0 dex, +0.3 dex, +0.5 dex.

We have also used the grid of MARCS model atmosphere (Gustafsson et al. 2008).These models are hydrostatic and computed on the assumptions of Local Thermodynamic Equilibrium (LTE), chemical equilibrium, homogeneous plane-parallel stratification, and the conservation of the total flux (radiative plus convective; the convective flux being computed using the local mixing length recipe). The radiation field used in the model generation is calculated by assuming absorption from atoms and molecules by opacity sampling at approximately 100000 wavelength points over the range 1300 Å to 20 μm. This grid spans effective temperatures between $2550\,\mathrm{K} < T_{\mathrm{eff}} < 4050\,\mathrm{K}$ in steps of 100 K, surface gravities of $5.0 < \log g(\mathrm{cgs}) < 5.5$ in steps of 0.5 dex, a constant microturbulence of $2\,\mathrm{km\,s^{-1}}$, and metallicities of $-0.5 < [\mathrm{Fe/H}] < 0.25$ in steps of 0.25 dex and with an $[\alpha/\mathrm{Fe}] = +0.2$ and +0.1 for the two lowest metallicities, respectively.

The model spectra are converted to absolute fluxes (erg $\mathrm{cm^{-2}\ s^{-1}\AA^{-1}}$) at the position of the observer by multiplying with the dilution factor $[r/d]^2$ where the stellar radii are varying from $0.096R_\odot$ to $0.142R_\odot$ at a step of 0.002 by assuming the distance for the system 7.72 pc (Costa et al. 2005).

3 Physical Parameters Determination and Results

3.1 Effective Temperature and Radius

The effective temperature and radius have been calculated using a χ^2 minimization technique in an automatic interactive way in IDL program. In this technique we first rebin all the synthetic spectra both in optical and infrared to the same resolution as the observed spectra. For all of the observed spectra we then calculate the χ^2 value compared to the grid of the synthetic spectra in the wavelength range between 4500 Å to 2.4 μm . Due to the low S/N ratio of the observed spectra, we excluded the region below 4500 Å. In a second step a 3-D χ^2 map has been obtained for each of the component in the optical and in infrared as a function of temperature and radius. The 3-D χ^2 plot both in optical and in IR shows clearly the parameter space which gives an acceptable solution. We then compared the possible solutions in the optical and IR for each component. The common intersection between the solutions in the optical and infrared were considered as the best physically acceptable solution. The solution was then crossed checked by visual inspection by overploting them with the observed spectra. The same procedure has been used with both BT-Settl and MARCS model. The derived parameters are given in Table 1. Figure 1 shows the best fit model superimposed to the observed optical and IR spectra for all the three components using BT-Settl and MARCS model.

3.2 Gravity and metallicity

Assuming the stellar radii from theoretical evolutionary model (Baraffe et al. 1998; Baraffe 1999), and the masses computed by Seifahrt et al. (2008), the log g of the components is found to be close to 5.3. We therefore

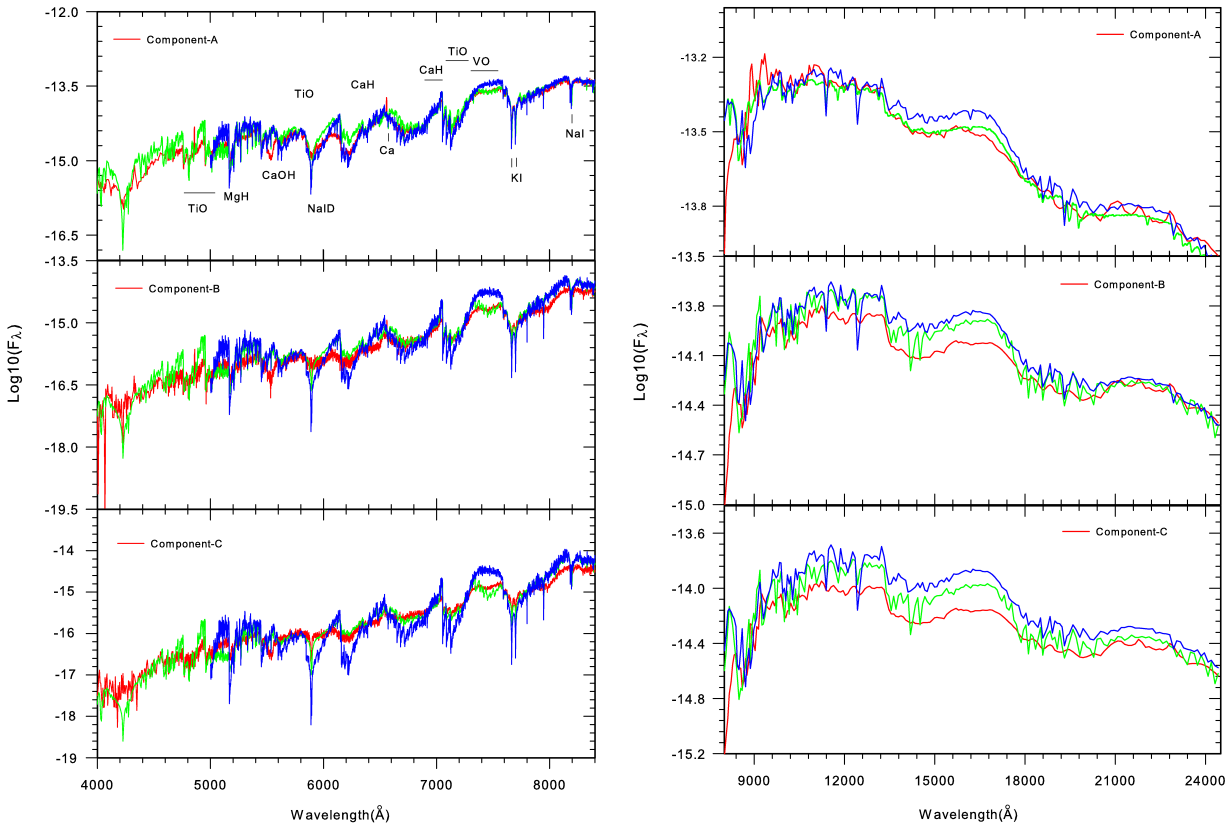

Fig. 1. Optical (left) and Infra-red (right) spectra of all three components. Red: observed spectra. Green: best fit BT-Settl model. Blue: best fit MARCS model. The parameters that give the best fit are given in Table 1.

Table 1. Derived parameters for the LHS1070 system. The uncertainties are drawn from the χ^2 maps and is 100 K for T_{eff} . The metallicity is assumed to be [m/H] = 0 and log g = 5.0 to 5.5

Component	Spec. Type	BT-Settl model				MARCS model		
		[m/H]	T_{eff} (K)	log g	Radius ($R_\odot$)	T_{eff} (K)	log g	Radius ($R_\odot$)
A	M5.5-M6	0.0	2900	5.5	0.134±0.005	2900	5.0	0.136±0.005
B	M8.5	0.0	2500	5.5	0.102±0.004	2600	5.0	0.098±0.002
C	M9.5-M9	0.0	2400	5.5	0.098±0.002	2500	5.0	0.100±0.002

restrict our analysis with gravity of 5.0 and 5.5 dex. The surface gravity can be obtained by analyzing the atomic line like K I, Na I and metal hydride like CaH which are gravity sensitive. K I line line 7665 Å and 7699 Å is particularly useful gravity discriminant for M stars. The high density of low-mass stars cause an increase in the gravity and thus the pressure broadening will enhanced the line profiles. Figure 2 (left panel) shows such determination of the gravity for the component A from K I line using both BT-Settl and MARCS model. The strength of line suggests that some important dust opacities yet has to be included into the model. The best fit gives us a log g = 5.5 for the BT-Settl models while log g=5.0 for the MARCS models. However both values agree within the uncertainties as found by Seifahrt et al. (2008).

The main indicator of the metallicity for all three component is the VO absorption band 7300 Å– 7600 Å which is very well reproduced by the BT-Settl model for the solar metallicity for all the components (see Figure 2, right panel).

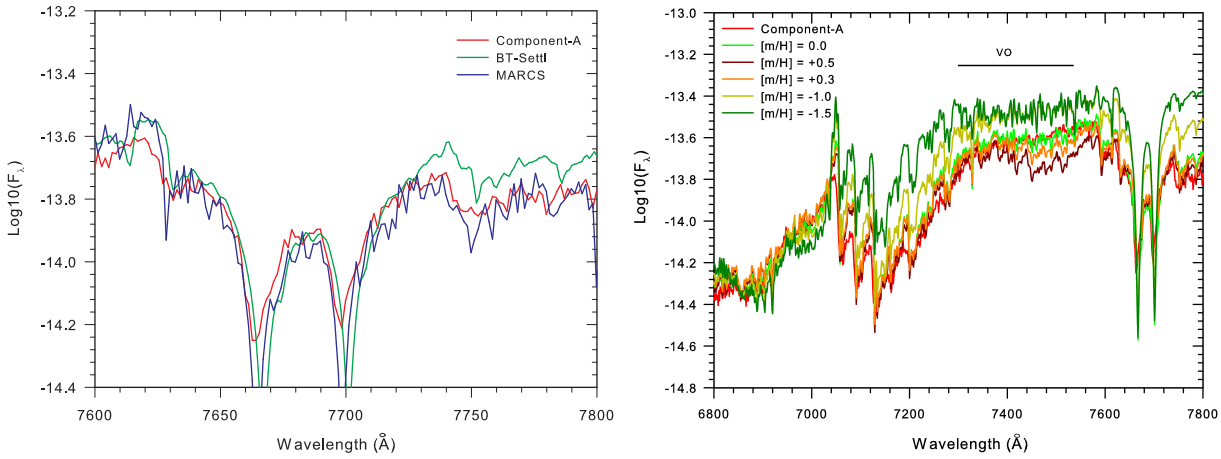

Fig. 2. Left: KI line in the component A (red) compared to the BT-Settl model (green) at T_{eff} = 2900 K, log g = 5.5, $R_\odot$ = 0.134 at solar metallicity along with the MARCS model (blue) at T_{eff} = 2900 K, log g= 5.0, $R_\odot$ = 0.136 at solar metallicity. **Right:** VO band observed in the component A (red) compared to the BT-Settl model at T_{eff} = 2900 K, log g = 5.5, $R_\odot$ = 0.134 at different metallicity

4 Conclusions

This paper presents the results from the spectral synthesis analysis of the LHS1070 triple system. We have determined the physical parameters T_{eff}, log g , metallicity and radius of all the three component by comparing observed spectra with the synthetic spectra computed by BT-settl and MARCS models. The derived parameters agree with those derived using evolutionary models and observed bolometric luminosities (Baraffe et al. 1998; Chabrier et al. 2000). While for the hotter component A the overall agreement between the model and the spectra is satisfactory, we find systematic differences for model B and C. For both components the overall fit is better with the BT-Settl model than the MARCS model. However, we noticed several issues regarding the BT-Settl models. The MgH around 5200 Å, NaI doublet at around 5900 Å is far too strong as well as the CaH band at 7000 Å while the CaOH band is missing. On the other side the TiO and VO band strengths are well reproduced by the models in the NIR part but the calculated fluxes are too high mainly in the J and H band. This may be due to the consideration of too hot deep layers from which the fluxes emerges. This indicates an inaccuracy in the atmosphere structure and also the treatment of the dust grains and opacities in the models as effective temperature decreases which was already proposed by Leggett et al. (2001). There is also clearly a discrepancy in the predicted water bands mainly in the J and H-band visible. Thus LHS1070 can be used as a testbed to validate and define further developments of the atmospheric models.

We acknowledge financial support from "Programme National de Physique Stellaire" (PNPS) of CNRS/INSU, France

References

Allard, F., Alexander, D. R., & Hauschildt, P. H. 1998, in Astronomical Society of the Pacific Conference Series, Vol. 154, Cool Stars, Stellar Systems, and the Sun, ed. R. A. Donahue & J. A. Bookbinder, 63

Allard, F., Homeier, D., & Freytag, B. 2010, ArXiv e-prints astro-ph.SR 1011.5405

Asplund, M., Grevesse, N., Sauval, A. J., & Scott, P. 2009, ARA&A, 47, 481

Baraffe, I. 1999, in Astronomical Society of the Pacific Conference Series, Vol. 173, Stellar Structure: Theory and Test of Connective Energy Transport, ed. A. Gimenez, E. F. Guinan, & B. Montesinos, p. 111

Baraffe, I., Chabrier, G., Allard, F., & Hauschildt, P. H. 1998, A&A, 337, 403

Bean, J. L., Sneden, C., Hauschildt, P. H., Johns-Krull, C. M., & Benedict, G. F. 2006, ApJ, 652, 1604

Bonfils, X., Forveille, T., Delfosse, X., et al. 2005, A&A, 443, L15

Butler, R. P., Vogt, S. S., Marcy, G. W., et al. 2004, ApJ, 617, 580

Chabrier, G., Baraffe, I., Allard, F., & Hauschildt, P. 2000, ApJ, 542, 464

Costa, E., Méndez, R. A., Jao, W.-C., et al. 2005, AJ, 130, 337
Freytag, B., Allard, F., Ludwig, H.-G., Homeier, D., & Steffen, M. 2010, A&A, 513, A19
Gustafsson, B., Edvardsson, B., Eriksson, K., et al. 2008, A&A, 486, 951
Leggett, S. K., Allard, F., Geballe, T. R., Hauschildt, P. H., & Schweitzer, A. 2001, ApJ, 548, 908
Leinert, C., Allard, F., Richichi, A., & Hauschildt, P. H. 2000, A&A, 353, 691
Leinert, C., Jahreiß, H., Woitas, J., et al. 2001, A&A, 367, 183
Leinert, C., Weitzel, N., Richichi, A., Eckart, A., & Tacconi-Garman, L. E. 1994, A&A, 291, L47
Ludwig, H.-G., Allard, F., & Hauschildt, P. H. 2006, A&A, 459, 599
Seifahrt, A., Röll, T., Neuhäuser, R., et al. 2008, A&A, 484, 429
Tsuji, T., Ohnaka, K., Aoki, W., & Nakajima, T. 1996a, A&A, 308, L29
Tsuji, T., Ohnaka, K., Aoki, W., & Nakajima, T. 1996b, A&A, 308, L29